THE ASTROPHYSICAL JOURNAL, 416:372–378, 1993 October 10

THE SPECTRUM OF EZ CANIS MAJORIS (HD 50896) TO THE LYMAN LIMIT WITH THE HOPKINS ULTRAVIOLET TELESCOPE

STEPHAN R. MCCANDLISS,[1,2] RICHARD H. BUSS, JR.,[1] WILLIAM P. BLAIR,[1] CHARLES W. BOWERS,[3]
ARTHUR F. DAVIDSEN,[1] PAUL D. FELDMAN,[1] AND JEFFREY W. KRUK[1]
Received 1993 January 28; accepted 1993 April 21

ABSTRACT

A unique flux-calibrated spectrum, extending to the Lyman limit of the Wolf-Rayet star EZ CMa (also known as WR 6, HD 50896, spectral type WN5) has been recorded by the Hopkins Ultraviolet Telescope. We compare the spectrum to a pure He continuum model with the stellar parameters $L_* = 10^{5.2}\ L_\odot$, $R_* = 4.5\ R_\odot$, $T_{\rm eff} = 57{,}000$ K, $V_\infty = 1700$ km s^{-1}, and $\dot{M} = 10^{-4}$ yr^{-1}. These parameters are very close to those derived by Hamann et al. (1988) from quantitative spectroscopy of ultraviolet, visual, and infrared He emission lines (although they represent only one solution from a locus of solutions that scale with distance). After correcting for interstellar atomic and molecular H absorption, assuming a reddening of $E_{B-V} = 0.06 \pm 0.03$ and a distance of 2.1 kpc, we find the model is a fairly good representation of the visual and near-UV continuum flux, but it underestimates the flux at the Lyman limit by a factor of ≈ 1.5. The lower limit in E_{B-V} might account for this discrepancy. However, part of the discrepancy may also be due to blends of wind-broadened He II, N III–V, O VI, S III–IV and VI, P V, and Fe V–VI emission lines creating an elevated pseudo-continuum, an effect not accounted for in the pure He model. The precise balance of these two effects remains to be determined. We conclude that the model given above provides an adequate fit to the data.

Subject headings: line identification — stars: individual (EZ Canis Majoris) — stars: Wolf-Rayet — ultraviolet: stars

1. INTRODUCTION

The high photometric precision of the Hopkins Ultraviolet Telescope (HUT) allows us to address a long-standing question in Wolf-Rayet (W-R) star research; what is the far-ultraviolet (FUV) energy distribution of these stars at the Lyman limit? Recent advances in W-R star modeling (e.g., Hillier, 1987a, b; Hamann & Schmutz 1987; Wessolowski, Schmutz, & Hamann 1988; Hillier 1988) and the determination of intrinsic stellar parameters from line profile fits to these models (also known as quantitative spectroscopy; e.g., Hamann, Schmutz, & Wessolowski 1988; Schmutz, Hamann, & Wessolowski 1989; Howarth & Schmutz 1992) has proceeded without the constraint of observations below Lyman-α. These models generally assume the atmosphere is a pure He, spherically symmetric, monotonically expanding wind. The N-rich W-R star, EZ Canis Majoris (spectral type WN5), is the "Rosetta stone" which modelers seek to interpret. There are many reasons for this: at $v = 6.94$ in the narrow-band *uvbr* system of Smith (1968), it is one of the brightest W-R stars (van der Hucht et al. 1981); it has low reddening, as evidenced by the nearly complete lack of a 2200 Å feature (Howarth & Phillips 1986); it has a low ratio of H to He (Conti, Leep, & Perry 1983), and there is good agreement on its distance ($d = 2$ kpc [Howarth & Phillips 1986]; $d = 1.8$ kpc [Schmutz & Howarth 1991]). It is debatable whether this status as a "standard" is deserved: EZ CMa is a known variable, it may have an intrinsically unstable wind, and it may have a compact companion (see Robert et al. 1992 for a summary of its enigmatic nature). However, Schmutz (1991) argues that every W-R star observed with high precision exhibits some variability. He finds that a variation in v of 0.03 mag translates to a temperature change of $\approx 1\%$, which is well within the uncertainty of the models.

In this paper our purpose is to compare current knowledge of this star with the HUT observation. We have corrected the fluxed spectrum for interstellar atomic and molecular H absorption, identified the emission features below 1200 Å, dereddened with an average galactic extinction curve, and compared the result to a continuum model. The data acquisition and reduction procedures are discussed in § 2. The interstellar H and H_2 absorption correction and the emission-line identifications are given in § 3. The dereddening is described in § 4. The comparison to a continuum model provided by Schmutz (1992) is presented in § 5, where we also discuss the differences between the model and the dereddened spectrum. We conclude that the differences can be accounted for given the model's neglect of line blending and possible errors in the extinction determination.

2. THE OBSERVATION AND DATA REDUCTION

HUT was launched on 1990 December 2, as a component of the Astro-1 observatory located in the bay of the space shuttle Columbia. The f/2 telescope consists of an iridium-coated 0.9 m parabolic primary with a prime focus, osmium-coated, Rowland grating spectrometer that covers 830 to 1860 Å in first order with a dispersion of 0.51 Å pixel^{-1}. Details concerning the HUT instrumentation can be found in Davidsen & Fountain (1985). The in-flight calibration and performance is described in Davidsen et al. (1992). The spectrum of EZ CMa was recorded on the fourth day of the flight, starting at JD = +2,448,230.968 with the exposure lasting for 1096 s. The high FUV flux from this source would have exceeded the 5000 counts s^{-1} linearity limit of the detector (an image-intensified one-dimensional Reticon array), so a small door was used,

[1] Center for Astrophysical Sciences, Department of Physics and Astronomy, The Johns Hopkins University, Baltimore, MD 21218.
[2] Electronic mail: I: stephan@pha.jhu.edu.
[3] Postal address: NASA/Goddard Space Flight Center, Code 693, Greenbelt, MD 20771.

which reduced the total flux by a factor of 100. Problems with the Instrument Pointing System (IPS) caused the star to wander in and out of the spectrometer's 18″ circular aperture. However, the pointing was steady during the last 300 s of the observation, with the star completely contained within the aperture, and a reliable count rate was obtained. The effective integration time, after accounting for the image wandering was 603 s. The mean observed count rate for the entire observation was 771 counts s^{-1}

The unsteady pointing produced time-dependent shifts in the zero point of the wavelength scale, which we tracked by computing the line centroid changes of a bright emission feature (N v λ1240) in a time series of spectral scans binned at 2 s intervals. Four major zero-point shifts were identified, and the spectra were shifted and co-added accordingly. The absolute zero point of the final spectrum is uncertain by the 6 Å diameter of the aperture, so we have adopted the rest frame of the interstellar H_2 absorption features (see § 3) by shifting the co-added spectrum redward by 2 Å. These absorption features have a FWHM of $\approx$2.2 Å, which is slightly better than the $\approx$3 Å instrumental resolution given by Davidsen et al. (1992). Using the f/20 beam of the small door reduces the grating aberrations and yields the improved resolution.

The raw, unsmoothed count spectrum is displayed in Fig. 1, where we have marked the prominent emission features and the Fe v–vi emission band. The square root statistics realized by the photon-counting detector allows the spectrum's statistical significance to be immediately assessed. In Figures 2 and 3 we have applied a small door flat-field correction and converted from counts to flux (ergs s^{-1} cm^{-2} $Å^{-1}$) through a calibration based on HUT's observation of the pure hydrogen white dwarf G191-B2B and an atmospheric model of this star (Davidsen et al. 1992). The flux-calibrated spectrum has been smoothed with a 4 pixel (2.04 Å) boxcar average. We have cut off the spectrum at 1820 Å, which is where the Lyman edge starts to appear in second order. Contamination by second-order flux between 456 and 912 Å is unlikely; log $N_{\rm H\,I}$ (cm^2) = 20.7 (see § 3), yielding an optical depth of $\approx$500 at 500 Å. We have compared the portion of the HUT spectrum that overlaps the *IUE* spectrum of Howarth & Phillips (1986) and find an rms deviation of 10%, after excluding regions around the three deepest absorption troughs and smoothing by 4 pixels. The *IUE* spectrum is a compilation of several spectra; in view of the UV line profile variations reported by St-Louis et al. (1989), the agreement is very good.

3. INTERSTELLAR H I AND H_2 ABSORPTION AND STELLAR EMISSION-LINE IDENTIFICATION

Absorption of stellar flux by interstellar neutral and molecular H occurs in the FUV spectrum from Lyman-α to the Lyman edge, causing some emission features to appear shifted, split, or absorbed completely. Individual lines in the H_2 Lyman ($B^1\Sigma_u^+ - X^1\Sigma_g^+$) and Werner ($C^1\Pi_u^\pm - X^1\Sigma_g^+$) absorption systems are unresolved by HUT, appearing as semiregularly spaced bands. The Lyman series of H I appears as discrete absorption features starting at Lyman-α, which gradually converge and attenuate the flux toward the Lyman edge. Column densities of H_2 and H I toward EZ CMa have been determined from *Copernicus* observations: log N_{H_2} = 19.3 from Shull (1977) and log $N_{\rm H\,I}$ = 20.57 from Bohlin, Savage, & Drake (1978) (units are number per cm^2 in dex). Shull (1977) found most of the H_2 in the first two rotational levels of the ground vibrational state, [log $N(J = 0)$ = log $N(J = 1)$ = 19.0, accurate to 30%], at a temperature of 80 K. The upper levels (J = 3, 4, 5) were found to be overpopulated. Bohlin et al. (1978) determined the neutral H column density by nulling the broad, fully damped absorption wings of Lyα to a "continuum" level (e.g.,

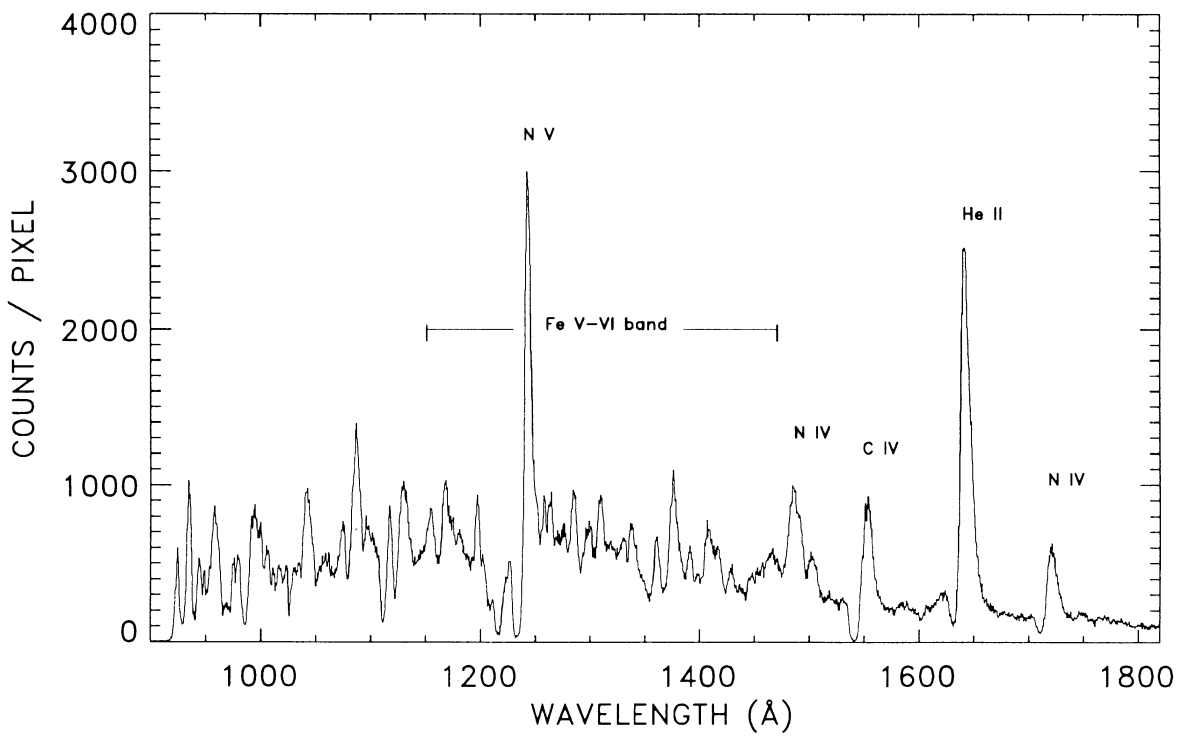

FIG. 1.—The raw and unsmoothed HUT spectrum of EZ CMa in counts per 0.51 Å pixel

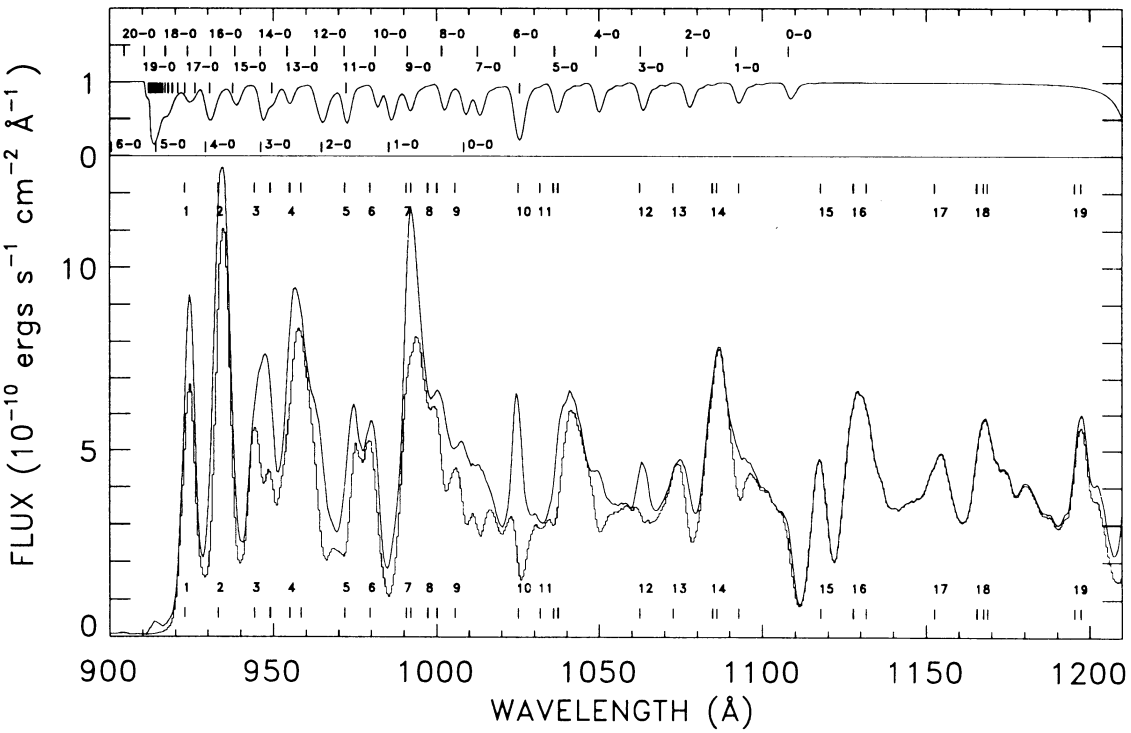

FIG. 2.—The fluxed spectrum both uncorrected and corrected for interstellar atomic and molecular H absorption. The upper panel is the continuum-normalized synthetic absorption spectrum of H I and H_2. The ticks mark the Lyman and Werner band heads of H_2 and the Lyman series of H I. The lower panel shows the fluxed HUT spectrum (*stepped line*) and the spectrum corrected for H absorption (*smooth line*). The spectra have been smoothed by 4 pixels (2.04 Å). The numbered tick marks in the lower panel refer to the lines listed in Table 1.

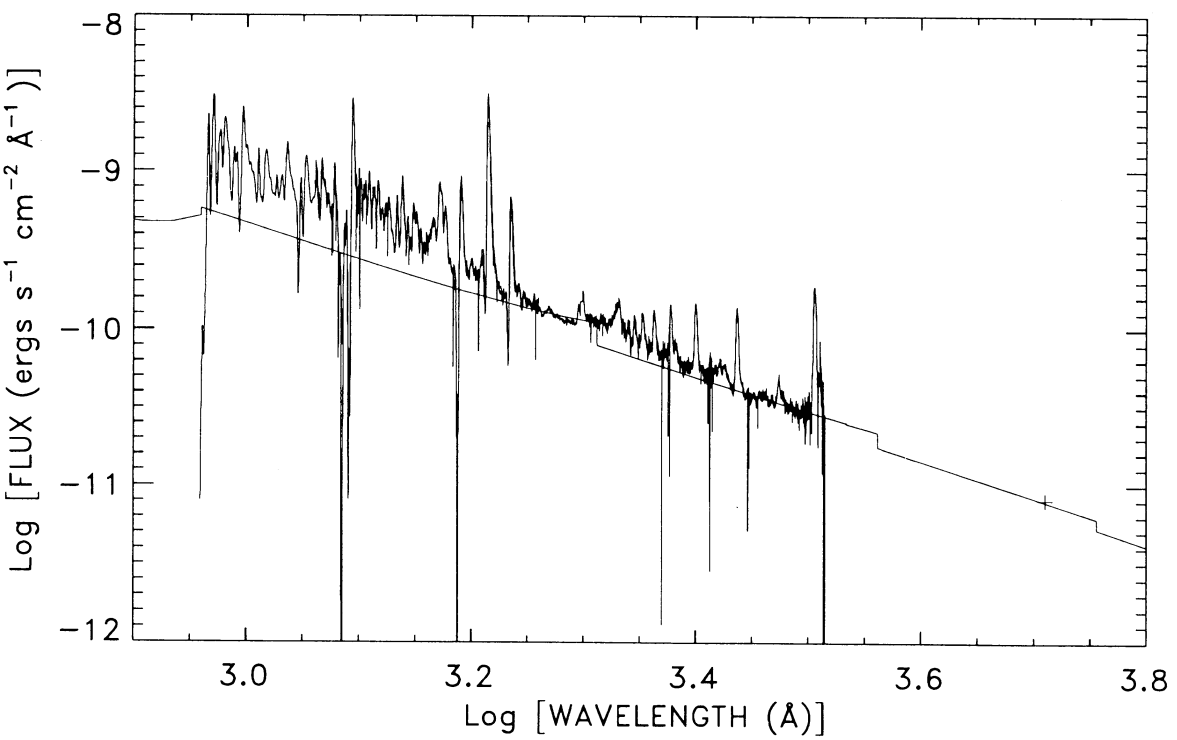

FIG. 3.—The dereddened and H absorption–corrected spectrum of EZ CMa from 912 to 5160 Å compared to a continuum model. The large downward spikes are either troughs of P Cygni profiles or reseau marks. See text for details.

Bohlin 1975). Howarth & Phillips (1986) point out this underestimates the H I column density because no account is made for the very strong He II Balmer-β line at λ1216 which is certain to be present based on the strength of the He II Balmer-α line at λ1640. They have determined a slightly higher column, log $N_{\rm H\,I} = 20.7$, to account for this effect.

In an effort to provide a clearer picture of the emission features intrinsic to the star we constructed a synthetic spectrum of the molecular and atomic H absorption features to divide into the HUT spectrum. The atomic data for 420 Lyman and Werner lines of H_2 were taken from Morton & Dinerstein (1976) and the atomic data for the first 49 lines of the Lyman series were computed from Allen (1976). Below we follow the notation of Cartwright & Drapatz (1970). The line profile of each line was calculated on a fine-wavelength mesh by multiplying the line core optical depth (τ_0) by the Voigt profile [$H(a, x)$] and taking a negative exponential $e^{-\tau_0 H(a,x)}$; x is the frequency in Doppler units , and a is the ratio of line damping constant to Doppler width. The individual line profiles were then linearly interpolated to a common intermediate-wavelength mesh and multiplied together to form the combined synthetic spectrum. The intermediate spectrum was convolved with a 2.2 Å (FWHM) Gaussian point-spread function and finally rebinned to the HUT 0.51 Å wavelength mesh. A Doppler width of 10 km s^{-1}, a temperature of 80 K, a log $N_{\rm H\,I} = 20.7$, and a log $N_{\rm H_2} = 19.1$ were used. The reason for the smaller molecular H column is given below. The resolution here is inadequate to address the question of upper rotational level overpopulation in H_2. A redetermination of the neutral H column awaits a satisfactory procedure for removing geocoronal Lyman-α from the line core; we will defer this to a later study. The synthetic H I + H_2 absorption spectrum, the uncorrected HUT spectrum, and the absorption corrected HUT spectrum are plotted in Figure 2.

The effects of neutral and molecular H absorption are gross. For instance, the combination of Lyman-β and Lyman (6–0) has effectively removed He II Balmer δ at 1025 Å and Lyman (3–0) has removed S IV λ1602. S VI λ944 is split by Lyman δ, Lyman (14–0) and Werner (3–0). The blueward wing of O VI $\lambda\lambda$1032–1037 is suppressed by Lyman (5–0). The region below 950 Å is gradually attenuated by the convergence of the H I Lyman series. Our synthetic spectrum appears to undercorrect Lyman (1–0) absorption while slightly overcorrecting the Werner (0–0) and Lyman (7–0) absorption blend. To balance this discrepancy, we chose the lower limit to the H_2 column (log $N_{\rm H_2} = 19.1$) given by Shull (1977). The apparent overcorrection of the Lyman (4–0) may be accounted for by the presence of strong Ar I absorption at λ1048 recorded by Shull (1977), which implies the redward side of the 1037 Å feature is stronger than depicted.

Emission lines from the Lyman limit to 1200 Å are displayed in the bottom panel of Figure 2. Each number (1–19) identifies an emission feature. In Table 1 we have listed the wavelengths of the peaks as measured from the H-corrected spectrum, along with the ions, the laboratory wavelengths, and the specific transitions, which potentially contribute to each feature. The ticks in Figure 2 mark the laboratory wavelengths of the suggested transitions. The wavelengths were measured by finding the line centroid of the line in a region surrounding the line peak. In identifying emission lines, preference was given to resonance transitions of astrophysically important atomic species with ionization potentials between 35 and 140 eV. We have also identified some N IV transitions that Hillier (1988) showed were pumped by continuum fluorescence, an excitation of upper level states by resonant absorption of extreme UV (EUV) He II continuum flux. The *Copernicus* spectrum of Johnson (1978) was used as a guide to the lines between 1012 and 1200 Å, while the identifications below 1012 Å are new.

TABLE 1

LINE IDENTIFICATIONS 912–1200 Å

Line	$\lambda_{\rm mea}$ (Å)	Ion	$\lambda_{\rm lab}$ (Å)	Transition
1	924.3	N IV	923.2	$2p^2\,^3P$–$2s2p\,^3P^o$
2	934.4	S VI	933.4	$3p\,^2p^o$–$3s\,^2S$
3	946.8	S VI	944.5	$3p\,^2P^o$–$3s\,^2S$
		He II	949.3	$10d\,^2D$–$2p\,^2P^o$
4	957.5	N IV	955.3	$2p^2\,^1S$–$2s2p\,^1P^o$
		He II	958.7	$9d\,^2D$–$2p\,^2P^o$
5	974.7	He II	972.1	$8d\,^2D$–$2p\,^2P^o$
6	979.8	N III	979.9	$2p^3\,^2D^o$–$2s2p^2\,^2D$
7	992.9	N III	991.0	$2s2p^2\,^2D$–$2s^2p\,^2P^o$
		He II	992.4	$7d\,^2D$–$2p\,^2P^o$
8	1000.1	P V	997.6	$4p\,^2P^o$–$3d\,^2D$
		P V	1000.4	$4p\,^2P^o$–$3d\,^2D$
9	1007.3	N III	1006.0	$2p^3\,^2P^o$–$2s2p^2\,^2S$
10	1024.7	He II	1025.3	$6d\,^2D$–$2p\,^2P^o$
11	1041.8	O VI	1032.0	$2p\,^2P^o$–$2s\,^2S$
		N IV	1036.2	$2s^4f\,^3F^o$–$2s3d\,^3D$
		O VI	1037.6	$2p\,^2P^o$–$2s\,^2S$
12	1063.5	S IV	1062.7	$3s3p^2\,^2D$–$3s^23p\,^2P^o$
13	1074.6	S IV	1073.0	$3s3p^2\,^2D$–$3s^23p\,^2P^o$
14	1086.8	He II	1085.0	$5d\,^2D$–$2p\,^2P^o$
		N IV	1086.4	$2s4s\,^3S$–$2s3p\,^3P^o$
		N IV	1093	$2p3d\,^3P^o$–$2s3d\,^3D$
15	1117.4	P V	1118.0	$3p\,^2P^o$–$3s\,^2S$
16	1129.8	P V	1128.0	$3p\,^2P^o$–$3s\,^2S$
		N IV	1131.9	$2p3p\,^3P$–$2s3p\,^3P^o$
17	1154.1	Fe VI	1152.8	$3d^24p\,(^1G)^2F_{5/2}$–$3d^24s\,(^1G)^2G_{7/2}$
18	1168.0	Fe VI	1165.7	$3d^24p\,(^3P)^2P_{3/2}$–$3d^24s\,(^3P)^2P_{3/2}$
		Fe VI	1167.7	$3d^24p\,(^1G)^2F_{7/2}$–$3d^24s\,(^1G)^2G_{9/2}$
		N IV	1169.0	$2p3d\,^3D^o$–$2s3d\,^3D$
19	1197.5	N IV	1195.6	$2s4p\,^3P^o$–$2s3d\,^3D$
		S III	1197.5	$3s3p^3\,^3D^o$–$3s^23p^2\,^3P$

Below 1012 Å, we find N IV λ923; S VI $\lambda\lambda$933–945; N IV λ955 possibly blended with He II λ959, He II λ972, N III λ980; and a large blend composed of the resonance line N III λ991, He II λ992, P V $\lambda\lambda$998–1000, and N III λ1006. The detection of the S VI $\lambda\lambda$933–945 resonance doublet lends credence to the identification of S VI $\lambda\lambda$1975–1993 in the *IUE* spectrum by Willis et al. (1986). We also note the presence of two features where S VI $\lambda\lambda$2587–2618 would be expected in the *IUE* spectrum.

Above 1012 Å, the first emission line identified by Johnson (1978) is the O VI $\lambda\lambda$1032–1038 resonance multiplet. The measured position of this emission feature is significantly shifted redward from the laboratory wavelengths,[4] and there is no strong P Cygni absorption trough as seen in the *Copernicus* spectra of γ^2 Vel (WC8 + O7; Johnson 1978) and ζ Pup (O4 If; Morton & Underhill 1977). The apparent shift may be due a C II interstellar absorption line at λ1036, noted by Johnson (1978). In evolutionary calculations, Maeder (1983) finds the surface abundance of ^{16}O in early-type WN stars is down by more than an order of magnitude from that found in early-type O stars, so it seems reasonable to question whether O lines

[4] The measured position of the feature is 4.2 Å to the red of the O VI λ1037.6 rest wavelength (see Table 1). The rms deviation between the measured line positions and the laboratory wavelengths of all the features, excluding O VI, is 1.6 Å.

should even be present in EZ CMa. A possible alternative to the O VI identification is N IV λ1036, which should form as a recombination line since the upper level is not pumped by the continuum via a resonant absorption transition (Bashkin & Stoner 1975). Redward of this region we find the S IV $\lambda\lambda$1062–1073 resonance multiplet. The red member of this feature was identified by Johnson (1978), but the presence of the blue member was not noted by him because of the strong absorption by the molecular H Lyman (3–0) band.

We prefer to identify λ1085 as a blend of He II Balmer-γ (which we expect to be present based on the strength of the He II λ1640) and N IV λ1086 (as predicted by Hillier 1988), instead of the N II λ1084 resonance line identification of Johnson (1978). While it may be possible for a N II resonance line to be present in a WN5 star, the W-R spectral classification favors high-ionization N species in early types (WN3–WN9 $\leftrightarrow$ early–late). Willis et al. (1986) find the N II λ1842 line does not appear until WN7 and increases in strength at WN8, which makes the appearance of a N II feature at spectral type WN5 less likely. The redward wing of the λ1085 feature is extended, an indication that the N IV λ1093 line predicted by Hiller (1988) is present. The redward wing of P V λ1128 is also extended, an indication that the N IV λ1132 line also predicted by Hillier (1988) is present. The line at λ1152 was not identified by Johnson (1978), and he attributed the line at λ1167 to a blend of O IV, C III, S III, and N IV lines. We attribute these two features to the Fe VI lines λ1152 and $\lambda\lambda$1166–1167 (Ekberg 1975) with the latter lines blended with N IV λ1169, also predicted by Hillier (1988). The Fe VI identification extends the pseudocontinuum blend of Fe V–VI lines, found by Koenigsberger (1988) to run from $\lambda\lambda$1250–1470 down to λ1152 (see also Schmutz 1991).

Johnson (1978) found no evidence for C III λ1176, and we agree. If it were present, we would expect to see the C III resonance line at λ977. If C III λ977 is present, it is blended with He II λ972 and N III λ980. It is not possible to rule out completely the presence of C III. However, it is clearly underabundant, so the C/N abundance estimate made by Hillier (1988), based on the assumption that all the C is C^{+++}, is probably justified. Finally, the feature at λ1197 has been identified by Johnson (1978) and Willis et al. (1986) as the resonance multiplet of S III $\lambda\lambda$1194–1201. This is puzzling because the ionization potential of this species is only 35 eV. As an alternative, we suggest this feature is N IV λ1196, another continuum fluorescence line with its upper state pumped by N IV λ791 (Moore 1971). The large number of broad emission features identified here makes it nearly impossible to identify the "continuum," and we conclude that line blending elevates the "effective continuum" to some degree.

4. REDDENING CORRECTION

Determinations of the reddening in EZ CMa range from $E_{B-V} = 0$ to 0.13 (Vacca & Torres-Dodgen 1990). This reddening is low enough to be plagued by a combination of intrinsic photometric variation and the difficulty in determining the intrinsic colors of WN-type stars. Kuhi (1967) reports variation of $\approx$0.4 mag for EZ CMa, in a 50 Å bandpass centered on 5556 Å for 33 measurements observed over 2 yr (1964–1965). Robert et al. (1992) report night-to-night continuum variations as large as 0.1 mag over several 1–4 month observing runs. The spread in the reported E_{B-V} is not surprising given this short- and long-term variation.

Recently a number of new methods for determining E_{B-V} have been applied to large W-R color data bases (cf. Vacca & Torres-Dodgen 1990, Conti & Morris 1990, and Schmutz & Vacca 1991). In particular Schmutz & Vacca (1991) find an $E_{B-V} = 0.06$ for EZ CMa by relating W-R intrinsic colors to the 3645 Å discontinuity predicted from the pure He W-R models of Schmutz et al. (1991). Unfortunately, their estimated error for the entire data set is $\pm$0.07 mag for color excesses $\leq$1 mag. However, their color excess for EZ CMa may be more accurate than $\pm$0.07 mag. An $E_{B-V} = 0.06$ is consistent with the color excess found by Howarth & Phillips (1986) for two nearby B stars which are also at 2 kpc: HD 51285 ($E_{B-V} = 0.062 \pm 0.017$) and HD 51854 ($E_{B-V} = 0.073 \pm 0.010$). These values are arithmetic means from different observers, and the errors are 1 standard deviation. For discussion purposes we will adopt an error of approximately $\pm$0.03 for the E_{B-V} to EZ CMa (this is 3 σ for HD 51854 and a little less than 2 σ for HD 51285).

The piecewise analytic interstellar extinction curve of Seaton (1979), with $R_V = 3.2$, extrapolated to the Lyman edge, was used to deredden the EZ CMa spectrum. We note Seaton's extrapolated FUV extinction curve is not too different from the polynomial extrapolation of Savage & Mathis (1979) used by Longo et al. (1989) to study the FUV energy distribution of *Voyager* OB-star spectra. The flux corrections for EZ CMa by these two curves differ by no more than 2%. A potentially more serious source of systematic error is the use of an average galactic extinction curve, as has been cautioned against by Garmany, Massey, & Conti (1984).

The complex physical environment of EZ CMa provides a variety of mechanisms that could cause deviations from the galactic average. For instance, EZ CMa is surrounded by the ring nebula S308, a wind-blown bubble about a half-degree in diameter (Johnson & Hogg 1965; Chu et al. 1982). The environment is further complicated by the presence of an old SNR in front of EZ CMa, some 3–4° in extent and at a distance of about 0.8 kpc, which Howarth & Phillips (1986) found from an analysis of high-velocity absorption features observed in the spectra of B stars along this line of sight. Seab & Shull (1983) have found that shock processing of interstellar dust, as might be expected at a wind/ISM interface, can cause preferential destruction of large grains, producing an increase in the strength of the 2200 Å bump and the FUV upturn. However, Howarth & Phillips (1986) point out that the material in the immediate vicinity of EZ CMa is only about 1% of the total material along the line of sight. From this we conclude that any deviations from the galactic average will be intrinsic to the line of sight rather than caused by the local environment. Since we have no detailed knowledge of the FUV extinction along this line of sight, we have resorted to the galactic average. A systematic FUV extinction study of the many B-type stars along this line of sight could help answer whether our assumption of a galactic average is valid.

5. COMPARISON AND CONCLUSIONS

In Figure 3 we show the log-log plot of flux as a function of wavelength for a combined HUT and *IUE* spectrum, along with Howarth & Schmutz's (1992) correction to Smith's (1968) v continuum flux at 5160 Å of $v^c = 6.88$. The stellar flux has been dereddened with an $E_{B-V} = 0.06$. We also show in this figure a model of the continuum flux based on the stellar parameters determined by Hamann et al. (1988) from UV,

visual, and infrared emission lines. Their method uses a grid of WN-type model atmospheres, calculated by Schmutz et al. (1989), from which the temperature, luminosity, mass-loss rate, and terminal velocity can be determined from profile fits to He I and II lines and a knowledge of the absolute visual magnitude (i.e., the distance and reddening). The model assumes a spherically symmetric, expanding atmosphere of pure He with a velocity law of the form $V_\infty[1 - (R_*/r)]^\beta$ with $\beta = 1$, where $R_* < r < \infty$ and V_∞ is the terminal velocity.[5] The pure He assumption is consistent with the H/He < 0.1 found by Conti et al. (1983) for this star. The parameters of the model are $L_* = 10^{5.2}\ L_\odot$, $R_* = 4.5\ R_\odot$, $T_{\rm eff} = 57{,}000$ K, $V_\infty = 1700$ km s^{-1}, and $\dot{M} = 10^{-4}\ M_\odot\ {\rm yr}^{-1}$. For comparison the parameters determined by Hamann et al. (1988) are $L_* = 10^{5.3}\ L_\odot$, $R_* = 4.7\ R_\odot$, $T_{\rm eff} = 57{,}500$ K, $V_\infty = 1700$ km s^{-1}, and $\dot{M} = 10^{-4}\ M_\odot\ {\rm yr}^{-1}$. These particular model parameters require a distance of 2.1 kpc to fix the flux at 5160 Å. However, we must emphasize that this distance and these model parameters are not unique, since it is possible to scale the model to any distance with the relations given in Howarth & Schmutz (1992) (eqs. [1], [2], and [3]), and $M(v^c) = v^c - R_v E(b - v) - 5 \log (D/10)$, where D is the distance in kpc and R_v is given in Schmutz & Vacca (1991) (see also Schmutz et al. 1989).

Figure 3 shows the model is a reasonable fit to the dereddened stellar spectrum in the visual and near-UV. Blueward of 3100 Å the discrepancy between the model and the stellar spectrum gradually increases until the He II n–3 increment at 2050 Å is reached; blueward from this edge, the spectrum follows the model. This is an example of how a pseudocontinuum is formed by the merger of the He II n–3 series of emission lines at the level 3 ionization edge (Schmutz & Vaca 1991). From the 2050 Å increment the discrepancy again increases toward the FUV, where at the Lyman edge the model is too low by a factor of $\approx$1.5. Given the large number of broad emission features identified between 912 and 1200 Å in § 3, we suspect that a pseudocontinuum has been formed throughout the FUV by the blending of lines, an extension of what Koenigsberger (1988) found for the Fe V–VI emission band between λ1250 and λ1470.

However, line blending alone may not be enough to account for all of the discrepancies. Given the strong dependence of the resulting FUV flux on the assumed reddening law, we need to consider how the uncertainty in the extinction determination will affect our result. Assume for the moment that line blending is unimportant. If we use a lower $E_{B-V} = 0.03$, which is within the range of values that we found in § 4 to be plausible (and the distance is increased slightly), then the dereddened spectrum will follow the model in the FUV, but blueward of the 2050 Å increment the spectrum will be lower than the model. In this case a "fine tuning" of the assumed stellar parameters might be made, to decrease the size of the 2050 Å increment in the model (e.g., Hillier 1987a who has investigated how the continuum shape is affected by changes in luminosity, mass loss rate, and stellar radius). An alternative to changing the stellar parameters at the lower E_{B-V} is to deredden with an extinction curve that has a strong 2200 Å bump. This would increase the 2050 Å increment in the dereddened spectrum but not increase the FUV upturn. The inferred extinction curve for this alternative is different from the shock process extinction curves of Seab & Shull (1983) that have an increase in the strength of both the 2200 Å bump and the FUV upturn.

We conclude that when the uncertainty in the extinction determination is combined with the effects of line blending, the model produces a reasonable fit. It is quite possible that small adjustments of the assumed model parameters, combined with the inclusion of lines from atomic species identified here, will result in a satisfactory fit to the observations without having to resort to nonstandard reddening curves or a different E_{B-V}. The challenge to modelers is to include the lines and determine how much of the "effective continuum" is real and how much is "pseudo." The challenge to observers is to improve the accuracy of the extinction determination and determine whether the extinction deviates significantly from the galactic average by observing the many B stars along this line of sight. We hope these efforts will result in a more accurate calibration of the quantitative spectroscopic method of determining W-R star parameters and provide a better picture of the nature of the FUV extinction.

[5] This formulation of the velocity law is valid only above the sonic point (Castor, Abbott, & Klein 1975).

We would like to express our thanks to Werner Schmutz who kindly provided the W-R model used here and to Ian Howarth who kindly provided the *IUE* spectrum. This work was supported by NASA contract NSA 5-27000 to The Johns Hopkins University.

REFERENCES

Allen, C. W. 1976, Astrophysical Quantities (London: Athlone), 70
Bashkin, S., & Stoner, J. O., Jr. 1975, Atomic Energy Levels and Grotrian Diagrams, Vol. 1, Hydrogen I–Phosphorus XV (Amsterdam: North-Holland), 142
Bohlin, R. C. 1975, ApJ, 200, 402
Bohlin, R. C., Savage, B. D., & Drake, J. F. 1978, ApJ, 224, 132
Cartwright, D. C., & Drapatz, S. 1970, A&A, 443
Castor, J. I., Abbott, D. C., & Klein, R. I. 1975, ApJ, 195, 157
Chu, Y.-H., Gull, T. R., Treffers, R. R., Kwitter, K. B., & Troland, T. H. 1982, ApJ, 254, 562
Conti, P. S., Leep, E. M., & Perry, D. N. 1983, ApJ, 268, 228
Conti, P. S., & Morris, P. W. 1990, AJ, 99, 898
Davidsen, A. F., & Fountain, G. H. 1985, Johns Hopkins APL Tech. Dig., 6, 28
Davidsen, A. F., et al. 1992, ApJ, 392, 264
Ekberg, J. O. 1975, Phys. Scripta, 11, 23
Garmany, C. D., Massey, P., & Conti, P. S. 1984, ApJ, 278, 233
Hamann, W.-R., & Schmutz, W. 1987, A&A, 174, 173
Hamann, W.-R., Schmutz, W., & Wessolowski, U. 1988, A&A, 194, 190
Hillier, J. D. 1987a, ApJS, 63, 947
———. 1987b, ApJS, 63, 965
———. 1988, ApJ, 327, 822
Howarth, I. D., & Phillips, A. P. 1986, MNRAS, 222, 809
Howarth, I. D., & Schmutz, W. 1992, A&A, 261, 503
Johnson, H. M. 1978, ApJS, 36, 217
Johnson, H. M., & Hogg, D. E. 1965, ApJ, 142, 1033
Koenigsberger, G. 1988, Rev. Mexicana Astron. Af., 16, 75
Kuhi, L. V. 1967, PASP, 79, 57
Longo, R., Stalio, R., Polidan, R. S., & Rossi, L. 1989, ApJ, 339, 474
Maeder, A. 1983, A&A, 120, 113
Moore, C. E. 1971, Selected Tables of Atomic Energy Levels and Multiplet Tables N IV, N V, N VI, N VII (NSRDS-NBS 3, 4)
Morton, D. C., & Dinerstein, H. L. 1976, ApJ, 204, 1
Morton, D. C., & Underhill, A. B. 1977, ApJS, 33, 83
Robert, C., et al. 1992, ApJ, 397, 277
Savage, B. D., & Mathis, J. S. 1979, ARA&A, 17, 73
Schmutz, W. 1991, in IAU Symp. 143, Wolf-Rayet Stars and Interrelations with Other Massive Stars in Galaxies, ed. K. A. van der Hucht & B. Hidayat (Dordrecht: Kluwer), 39
———. 1992, private communication
Schmutz, W., Hamann, W.-R., & Wessolowski, U. 1989, A&A, 210, 236
Schmutz, W., & Howarth, I. D. 1991, in IAU Symp. 143, Wolf-Rayet Stars and Interrelations with Other Massive Stars in Galaxies, ed. K. A. van der Hucht & B. Hidayat (Dordrecht: Kluwer), 639
Schmutz, W., & Vacca, W. D. 1991, A&AS, 89, 259
Seab, C. G., & Shull, J. M. 1983, ApJ, 275, 652
Seaton, M. J. 1979, MNRAS, 187, 73P

Shull, J. M. 1977, ApJ, 212, 102
Smith, L. F. 1968, MNRAS, 140, 409
St-Louis, N., Smith, L. J., Stevens, I. R., Willis, A. J., Garmany, C. D., & Conti, P. S. 1989, A&A, 226, 249
Vacca, W. D., & Torres-Dodgen, A. V. 1990, ApJS, 73, 685
van der Hucht, K. A., Conti, P. S., Lundstrom, I., & Stenholm, B. 1981, Space Sci. Rev., 28, 227
Wessolowski, U., Schmutz, W., & Hamann, W.-R. 1988, A&A, 194, 160
Willis, A. J., van der Hucht, K. A., Conti, P. S., & Garmany, C. D. 1986, A&AS, 63, 417